International Journal of Natural and Engineering Sciences
Uluslararası Doğa ve Mühendislik Bilimleri Dergisi
E-ISSN: 2146-0086, 11 (1): 13-19, 2017. www.nobel.gen.tr

Active vibration suppression of a single-link smart flexible manipulator

Levent MALGACA* Mehmet UYAR Şahin YAVUZ
Department of Mechanical Engineering, Faculty of Engineering, Dokuz Eylül University, Izmir, Turkey

*Corresponding Author:
E-mail:levent.malgaca@deu.edu.tr

Received: February 25, 2017
Accepted: May 12, 2017

Abstract

Vibration control can be implemented to smart flexible stationary or nonstationary mechanical systems. Smart flexible manipulators are one of the most popular examples of non-stationary systems. In this study, the analysis of a single-link smart flexible manipulator with a piezoelectric actuator is studied. The finite element model of the smart flexible manipulator (SFM) is created in ANSYS/APDL software. The natural frequencies are determined by the modal analysis. Then the transient analysis is carried out to obtain the vibration responses by driving the manipulator with a trapezoidal motion. The PID control algorithm is integrated to the transient solutions of the SFM to suppress the residual vibrations. The uncontrolled and controlled vibration results are presented for various controller gains, stopping positions and motion times.

Keywords: Piezoelectric, Smart Flexible Manipulator, Active Vibration Control, PID Control

INTRODUCTION

Engineers design and use flexible manipulators (FM) in robotic applications due to several advantages such as faster system response, smaller energy consumption and requirement of smaller actuators. However, unwanted vibrations occur due to flexibility. Amplitudes of vibrations at the tip point of FM can be controlled and reduced by using different methods.

Modeling and control methods of FM are reviewed in the previous literature survey in [1, 2]. The essential modeling techniques and the sensors systems for their applications are presented. Control strategies in the literature reviews provide some possible issues for future studies [2, 3]. A smart flexible manipulator (SFM) consists of a link and a piezoelectric patch. Modelling of SFM is the first step to analyze the dynamic behaviors [4, 5]. In the past, various researchers proposed different techniques such as Assumed mode method and Euler-Bernoulli beam theory to obtain the dynamic model of the SFMs [6, 7, 8].

Residual vibration amplitudes of FM can be suppressed by using passive or active control. Passive vibration control can be achieved by motion commands [9, 10, 11]. Active vibration control requires the closed loop system and an external actuator. Piezoelectric materials are widely used for the active vibration control of smart structures [12–15]. The piezoelectric actuators and sensors on the surface of the SFM are bonded to suppress the vibration of SFM at tip point [10]. Experiments are needed to verify the theoretical results. The closed-loop technique is used for the position control of the SFM in [12].

Different control methods have been studied to suppress the vibrations of SFM. In [16], positive position feedback (PPF) controller is applied to the SFM to reduce end effector vibrations. A composite controller, which consists of a fuzzy sliding mode and a linear quadratic regulator (LQR) controllers, is designed in [6]. The linear and angular velocity feedback controllers, the positive position feedback and multi-mode controllers, the PD controller with the Lyapunov approach are the other examples of the composite control method [17–19]. A combination of feedforward and feedback control is applied to the SFM for the optimal trajectory planning [20]. The system identification method is studied in [17].

In this study, the main objective is to reduce the residual vibrations of the SFM with a piezoelectric patch. Simulations are performed by using ANSYS/APDL. The paper is organized as follows. The FE model of SFM is created in Section 2. The closed-loop control is analyzed in Section 3. Various PD controller gains are studied. Numerical results are presented for two different stopping positions and motion times in Section 4.

MODELING of SMART FLEXIBLE MANIPULATOR

The finite element (FE) model of the smart flexible manipulator (SFM) considered in this study is shown in Fig.1.

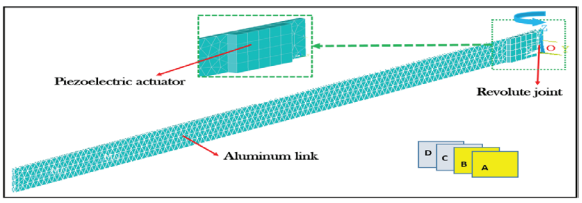


Figure 1. FE model of smart flexible manipulator

The FE model of the SFM is created by ANSYS/APDL software. The SFM consists of an aluminum link and a piezoelectric patch as shown in the figure. Material properties of the SFM are given in Table 1.

Table 1. Material properties

Piezoelectric actuator (PZT-5H), density: 7500 kg/m³			Aluminum link	
Elastic stiffness matrix (N/m²)	Piezoelectric strain matrix (C/m²)	Dielectric matrix (F/m)	Young's modulus (N/m²)	$69x10^9$
C_{11}=126.0 x10⁹ C_{12}=79.50 x10⁹ C_{13}=84.10 x10⁹ C_{33}=117.0 x10⁹ C_{44}=23.30 x10⁹	E_{31}=-6.5 E_{33}=23.3 E_{15}=17.0	ε_{11}=15.03x10^{-9} ε_{22}=15.03x10^{-9} ε_{33}=13.00x10^{-9}	Density (kg/m³)	2700

The dimension of the aluminum link and piezoelectric actuator is 500 mm x 20 mm x 2 mm, 25 mm x 20 mm x 3 mm, respectively. The piezoelectric patch is used as an actuator to suppress the residual vibrations of the manipulator. The piezoelectric patch is located at 10 mm away from the root. The surfaces C and D belong to the metal part and the surfaces A and B belong to the piezoelectric patch. Zero voltage is applied to common surfaces B and C as the ground voltage. The actuation voltage is applied to the surface A through the closed-loop control.

The FE model of the SFM is created using Solid226 elements. The metal part is modeled using Solid92 element while the piezoelectric patch is modeled using Solid226 element. Solid92 element has 5250 nodes with x, y, z displacement DOFs at per node. Solid226 element has 398 nodes with x, y, z displacement and voltage DOFs at per node. The FE model has 2506 elements and 5648 nodes in total.

The SFM rotates about the z axis. A revolute joint is defined at O to assign the motion to the SFM. A trapezoidal motion profile is used as shown in Fig.2

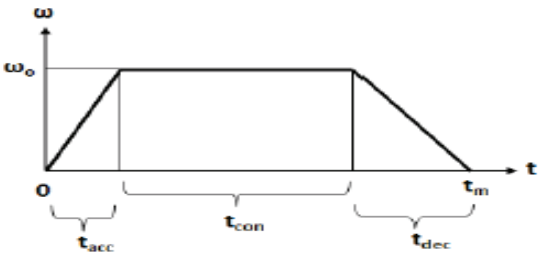


Figure 2. Trapezoidal velocity profile.

The parameters t_{acc}, t_{dec}, t_{con} are required to define the profile. t_{acc} is the acceleration time, t_{con} is the constant velocity time and t_{dec} is the deceleration time. The motion time t_m is found by summing these parameters t_{acc}, t_{dec}, t_{con}. The maximum angular velocity is calculated with the equation below.

$$\omega_0 = \frac{\theta_m \frac{\pi}{180}}{0.5t_{acc} + t_{con} + 0.5t_{dec}} \qquad (1)$$

Where, θ_m is the angular displacement in degree.

The motion parameters are defined as [t_{acc}, t_{con}, t_{dec}, t_m, θ_m] in the simulations. For practical applications in robotics, the values of tm and θ_m are known to move the manipulator [21, 22]. The user determines suitable values of the other motion parameters. Generally, the parameters t_{acc} and t_{dec} are selected as a percentage of t_m. If the values of t_{acc}, t_{dec}, t_m are known, then t_{con} is calculated from Eq. (1).

CLOSED-LOOP CONTROL

The natural frequencies should be determined before performing the analysis of the closed-loop control. Modal analysis is done to find the natural frequencies. The first three undamped natural frequencies and the corresponding bending mode shapes are shown in Fig.3.

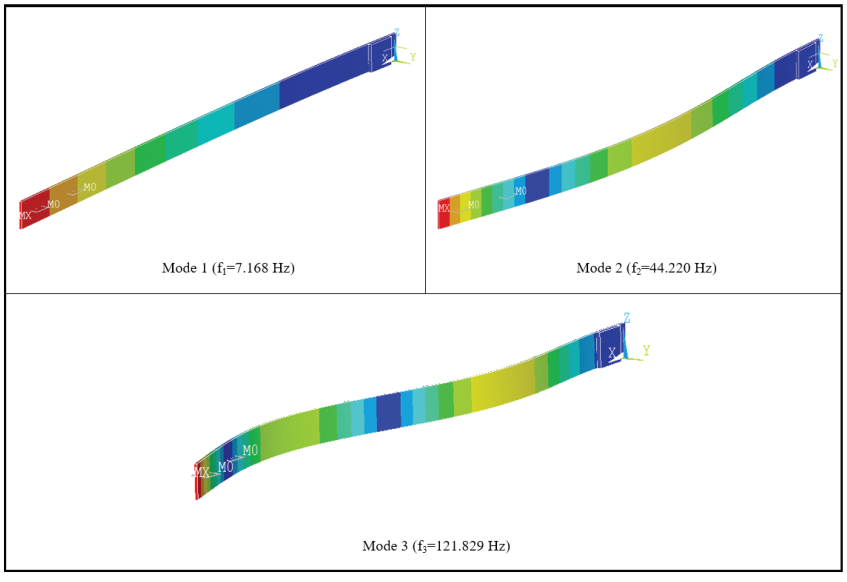


Figure 3. Undamped natural frequencies and mode shapes.

The time step δt and the settling time ts, which depend on the natural frequencies, are required to obtain the time responses of the SFM. The time step is calculated as $\delta t = 1/f_1/20$ by considering the first bending modes. The settling time is chosen as $t_s = t_m + t_{res}$, where tres is the time to obtain the residual vibrations after stopping the manipulator.

The block diagram for the closed-loop control is shown in Fig.4.

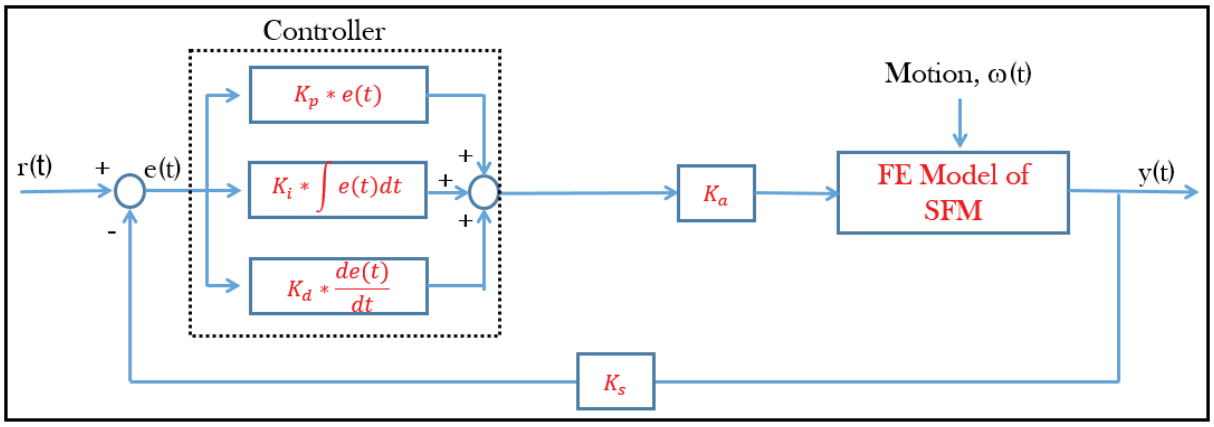


Figure 4. Closed-loop block diagram.

ω(t) is angular velocity assigning the revolute joint in order to move the manipulator. The vibrations during the motion and after the motion occur due to the flexibility. y(t) is the instantaneous values of the tip displacement of the manipulator K_s and K_a are the sensor and amplifier gains. The values of K_s and K_a are chosen as 250 and 30, respectively. The PID controller is used, and the controller gains K_p, K_i, K_d are the proportional, integral, and derivative gains, respectively. The instantaneous error value e(t) is calculated by subtracting the reference value from the sensor value. The error value is the input of the controller. The actuation signal is generated by multiplying the controller output and K_a. Then the actuation signal is applied to the piezoelectric actuator to suppress the residual vibration of the SFM. The controlled time responses of the SFM are obtained for various controller gains.

NUMERICAL RESULTS

Numerical results for the single-link SFM are obtained for two different t_m and θ_m. The values of t_m and θ_m are chosen as [2s, 4s] and [60º, 90º] in the simulations. The value of tres is chosen as 4s to obtain the residual vibrations. The example uncontrolled time responses of the SFM are shown in Fig.5 and Fig.6.

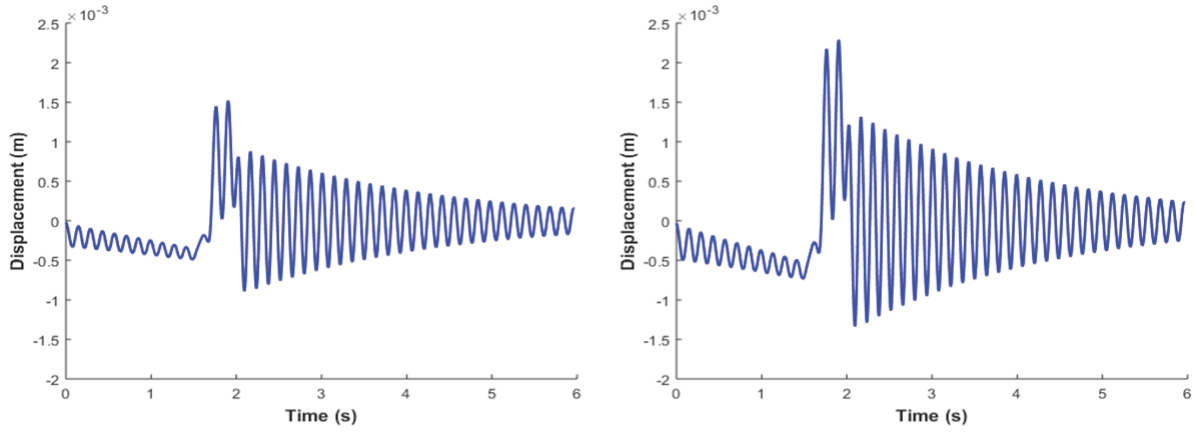
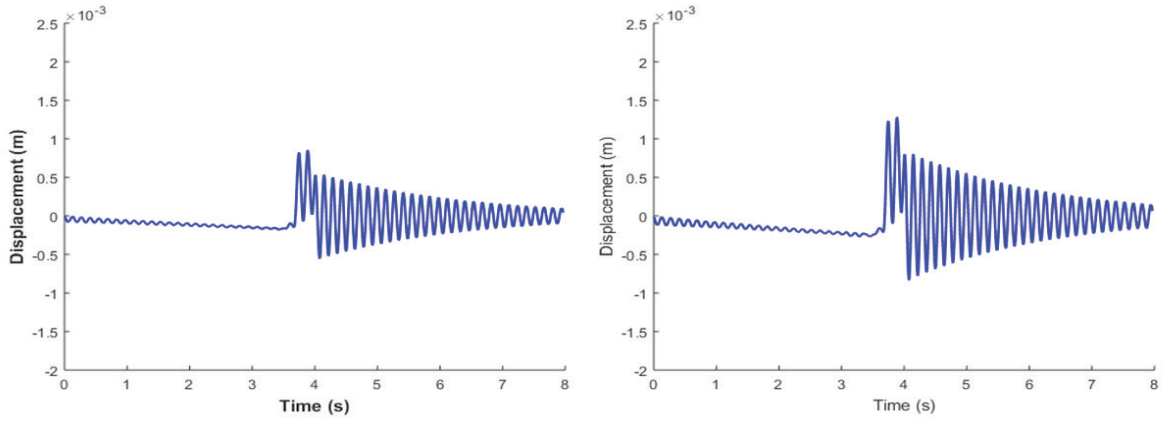


Figure 5. Uncontrolled time responses for (a) [1.5460, 0.1390, 0.3150, 2, 60], (b) [1.5460, 0.1390, 0.3150, 2, 90]

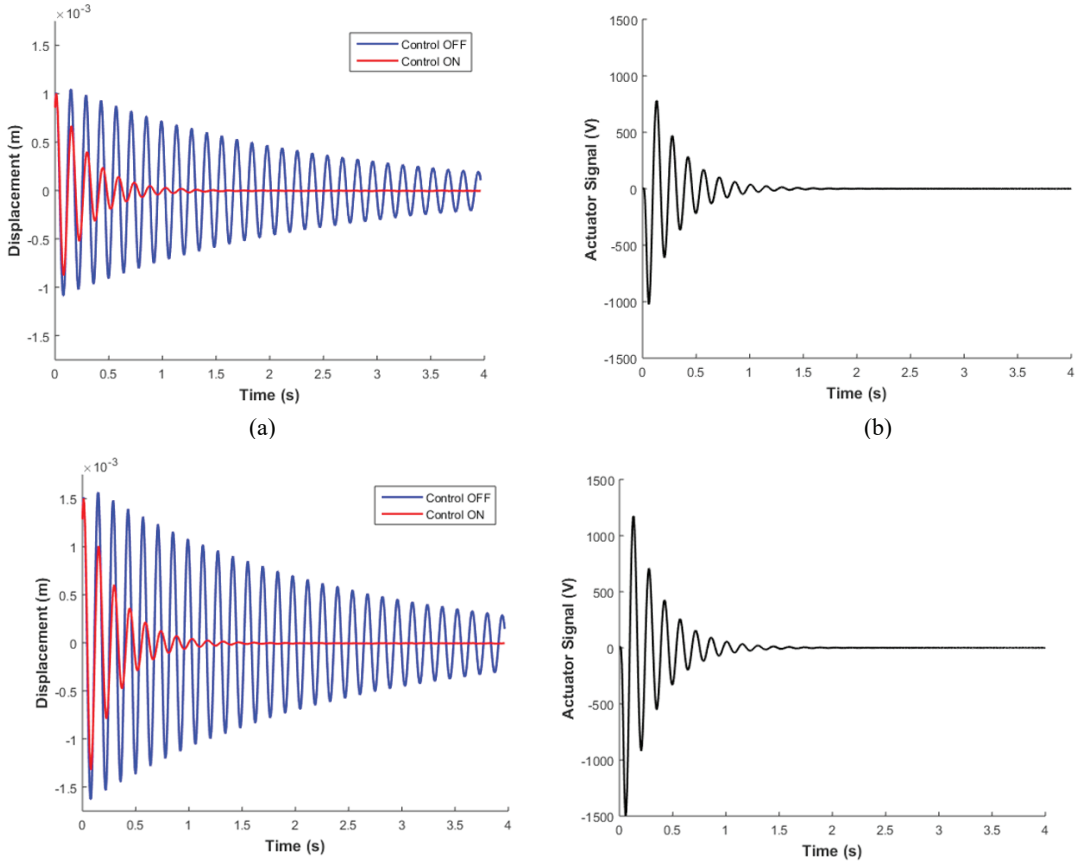


(a) (b)

Figure 6. Uncontrolled time responses for (a) [3.5460, 0.1390, 0.3150, 4, 60], (b) [3.5460, 0.1390, 0.3150, 4, 90]

In Fig. 5, the SFM moves to θ_m=60º and θ_m=90º for t_m=2s while the SFM moves to θ_m=60º and θ_m=90º for t_m=4s in Fig. 6. The free vibration, which is called as the residual vibration, starts after ending the motion of the SFM. It is observed that the residual vibrations increase as tm decreases and θ_m increases.

It is aimed to suppress the residual vibrations of the SFM through the active control as mentioned in Section 3. The residual parts of the vibration signals shown in Figs.5 and 6 of the SFM are evaluated at this stage. The example uncontrolled and controlled time responses of the SFM are shown in Fig. 7 and Fig. 8.



(a) (b)

(c) (d)

Figure 7. Uncontrolled and controlled time responses for K_p=100, K_d=2 with the motion of (a) [1.5460, 0.1390, 0.3150, 2, 60], (c) [1.5460, 0.1390, 0.3150, 2, 90]

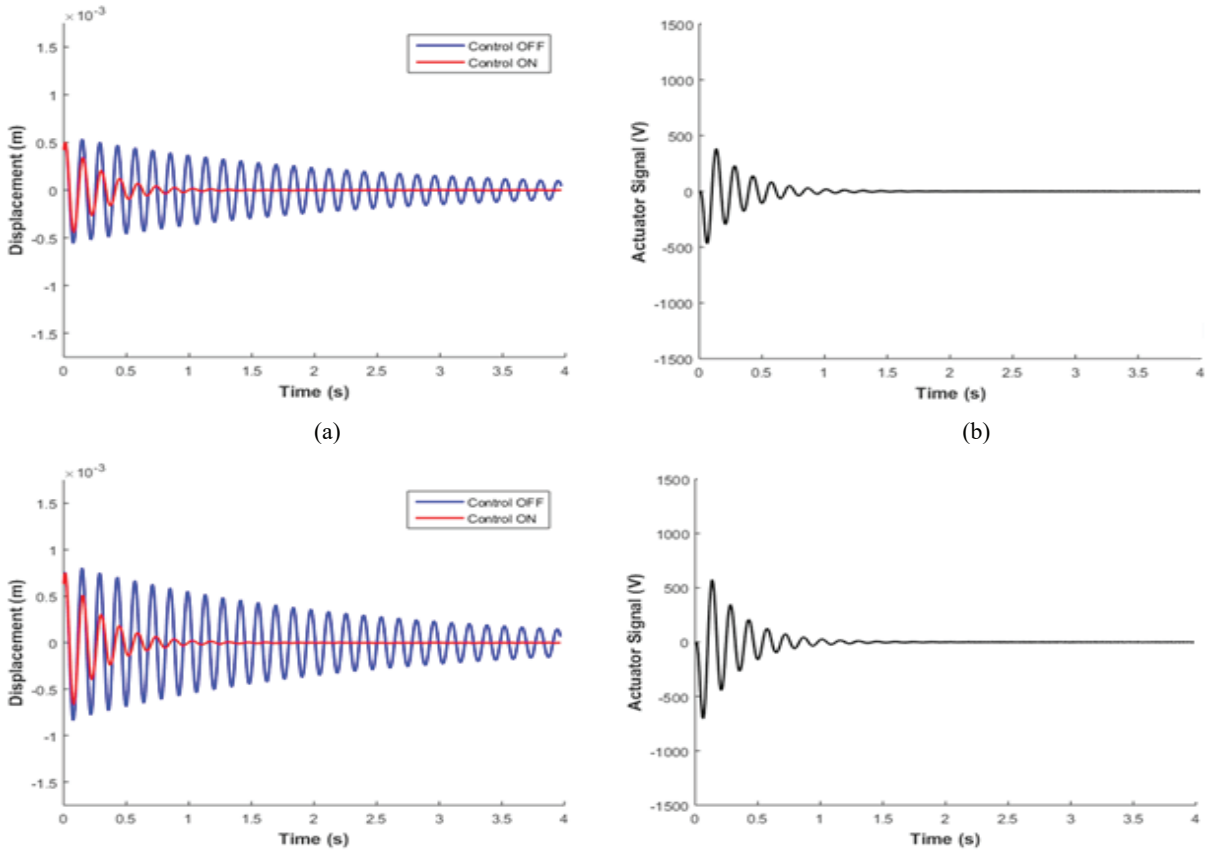


Figure 8. Uncontrolled and controlled time responses for K_p=100, K_d=2 with the motion of (a) [3.5460, 0.1390, 0.3150, 4, 60], (c) [3.5460, 0.1390, 0.3150, 4, 90]

It is observed from Fig.7 and Fig.8 that vibration suppression is achieved for different values of θ_m and t_m. The settling time decreases by the active control. Lower settling times require applying higher controller gains. Thus, the dynamic performance of the SFM can be improved and the SFM can be positioned more quickly.

Various controller gains are studied. The numerical results are given in Table 2. The root means square values y_{RMS}, the settling time t_s and damping ratio ζ of the residual vibrations are calculated to evaluate the effectiveness of the active control. The maximum actuation voltages V_{max}, which are applied to the piezoelectric actuator, are also listed in Table 2.

Table 2. Numerical results for the suppression of the SFM.

Motion parameters	Control gains		ζ	y_{RMS} (m)	t_s (s)	V_{max} (V)
	K_p	K_d				
[1.5460, 0.1390, 0.3150, 2, 60]	0	0	0.0088	$4.215x10^{-4}$	9.63	---
	40	0	0.0146	$3.322x10^{-4}$	5.54	324.54
	80	0	0.0225	$2.860x10^{-3}$	3.92	392.11
	100	0.75	0.0456	$2.093x10^{-4}$	2.02	745.25
	100	2	0.0788	$1.595x10^{-3}$	1.25	784.62
[1.5460, 0.1390, 0.3150, 2, 90]	0	0	0.0086	$6.324x10^{-4}$	9.36	---
	40	0	0.0145	$4.985x10^{-4}$	5.40	486.87
	80	0	0.0225	$4.292x10^{-4}$	3.91	967.12
	100	0.75	0.0456	$3.138x10^{-4}$	2.01	1118.0
	100	2	0.0785	$2.398x10^{-4}$	1.12	1179.63
[3.5460, 0.1390, 0.3150,4, 60]	0	0	0.0096	$2.142x10^{-4}$	9.50	---
	40	0	0.0144	$1.687x10^{-4}$	5.27	163.62
	80	0	0.0225	$1.448x10^{-4}$	3.77	327.63
	100	0.75	0.0451	$1.056x10^{-4}$	2.15	379.42
	100	2	0.0772	$0.806x10^{-4}$	1.18	400.78
[3.5460, 0.1390, 0.3150,4, 90]	0	0	0.0096	$3.210x10^{-4}$	9.22	---
	40	0	0.0140	$2.526x10^{-4}$	5.69	245.45
	80	0	0.0220	$2.175x10^{-4}$	3.91	491.45
	100	0.75	0.0452	$1.584x10^{-4}$	2.01	569.14
	100	2	0.0769	$1.206x10^{-4}$	1.25	601.20

It is observed from the table that vibration suppression can be achieved for various controller gains. The integral control gain is considered as K_i=0 for all cases. The values of y_{RMS} and t_s decrease as the values of control gain increase. The values of V_{max} increase as the values of control gain increase. The upper limit of V_{max} depends on the type and thickness of piezoelectric actuator [23].

CONCLUSIONS

The suppression of residual vibrations of an SFM is studied. The manipulator is moved with a trapezoidal motion. The motion profiles are generated for two different motion time and stopping positions. Numerical results obtained by ANSYS/APDL software are presented. The effect of the motion parameters and various controller gains are investigated. The residual vibrations of the SFM are successfully suppressed by using the PD controller.

REFERENCES

[1] M. Benosman and G. L.Vey, "Control of flexible manipulators : A survey," Robotica, vol. 22, no. October 2004, pp. 533–545, 2004.

[2] S. K. Dwivedy and P. Eberhard, "Dynamic analysis of flexible manipulators, a literature review," Mech. Mach. Theory, vol. 41, no. 7, pp. 749–777, 2006.

[3] C. T. Kiang, A. Spowage, and C. K. Yoong, "Review of Control and Sensor System of Flexible Manipulator," J. Intell. Robot. Syst. Theory Appl., vol. 77, no. 1, pp. 187–213, 2015.

[4] B. Bandyopadhyay, T. C. Manjunath, and M. Umapathy, Lecture Notes in Control and Information Sciences. NewYork Library: Springer-Verlag Berlin Heidelberg, 2007.

[5] D. Roy and G. V. Rao, Elements of Structural Dynamics Elements of Structural Dynamics. United Kingdom: John Wiley & Sons Ltd, 2012.

[6] E. Lu, W. Li, X. Yang, M. Fan, and Y. Liu, "Modelling and Composite Control of Single Flexible Manipulators with Piezoelectric Actuators," Shock Vib., vol. 2016, no. 2689178, 2016.

[7] K. Gurses, B. J. Buckham, and E. J. Park, "Vibration control of a single-link flexible manipulator using an array of fiber optic curvature sensors and PZT actuators," Mechatronics, vol. 19, no. 2, pp. 167–177, 2009.

[8] S. Choi, M. Seong, and S. H. Ha, "Accurate position control of a flexible arm using a piezoactuator associated with a hysteresis compensator," Smart Mater. Struct., vol. 22, no. 45009, p. 13, 2013.

[9] J. Shan, H. T. Liu, and D. Sun, "Modified input shaping for a rotating single-link flexible manipulator," J. Sound Vib., vol. 285, no. 1–2, pp. 187–207, 2005.

[10] K. Shin and M. J. Brennan, "Two simple methods to suppress the residual vibrations of a translating or rotating flexible cantilever beam," J. Sound Vib., vol. 312, no. 1–2, pp. 140–150, 2008.

[11] J. Shan, H.-T. Liu, and D. Sun, "Slewing and vibration control of a single-link flexible manipulator by positive position feedback (PPF)," Mechatronics, vol. 15, no. 4, pp. 487–503, 2005.

[12] M. Hassan, R. Dubay, C. Li, and R. Wang, "Active vibration control of a flexible one-link manipulator using a multivariable predictive controller," Mechatronics, vol. 17, no. 6, pp. 311–323, 2007.

[13] S. Khot, N. P. Yelve, R. Tomar, S. Desai, and S. Vittal, "Active vibration control of cantilever beam by using PID based output feedback controller," J. Vib. Control, vol. 18, no. 3, pp. 366–372, 2012.

[14] H. Karagülle, L. Malgaca, and H. F. Öktem,

"Analysis of active vibration control in smart structures by ANSYS," Smart Mater. Struct., vol. 13, no. 4, pp. 661–667, 2004.

[15] L. Malgaca, "Integration of active vibration control methods with finite element models of smart laminated composite structures," Compos. Struct., vol. 92, no. 7, pp. 1651–1663, 2010.

[16] J. C. P. Reis and J. S. d. Costa, "Design and experimental control of an active-flexible tubular manipulator link," J. Intell. Mater. Syst. Struct., vol. 23, no. 15, pp. 1741–1757, 2012.

[17] J. Lou, J. Liao, Y. Wei, Y. Yang, and G. Li, "Experimental Identification and Vibration Control of A Piezoelectric Flexible Manipulator Using Optimal Multi-Poles Placement Control," Appl. Sci., vol. 309, no. 7, p. doi:10.3390/app7030309, 2017.

[18] D. Sun, J. K. Mills, J. Shan, and S. K. Tso, "A PZT actuator control of a single-link flexible manipulator based on linear velocity feedback and actuator placement," Mechatronics, vol. 14, no. 4, pp. 381–401, 2004.

[19] R. Kumar, "Effective active vibration control of single link flexible manipulator with modified positive position feedback control in the presence of instrumentation phase lead/lag," J. Vib. Control, vol. 19, no. 10, pp. 1538–1560, 2012.

[20] J. Lou, Y. Wei, G. Li, Y. Yang, and F. Xie, "Optimal trajectory planning and linear velocity feedback control of a flexible piezoelectric manipulator for vibration suppression," Shock Vib., vol. 2015, 2015.

[21] L. Malgaca, Ş. Yavuz, M. Akdağ, and H. Karagülle, "Residual vibration control of a single-link flexible curved manipulator," Simul. Model. Pract. Theory, vol. 67, pp. 155–170, 2016.

[22] Yavuz, L. Malgaca, and H. Karagülle, "Vibration control of a single-link flexible composite manipulator," Compos. Struct., vol. 140, pp. 684–691, 2016.

[23] A. Preumont, Vibration control of active structures, 2nd ed. New York: Kluwer Academic Publishers, 2002.